# An Optimized Schwarz Waveform Relaxation Algorithm for Micro-Magnetics

Martin J. Gander[1], Laurence Halpern[2], Stéphane Labbé[3], and Kévin Santugini-Repiquet[1]

[1] University of Geneva, Section de mathématiques, Case Postale 64, 1211 Genève 4, Switzerland. {Kevin.Santugini,Martin.Gander}@math.unige.ch
[2] Institut Galilée, Université Paris 13, Département de mathématiques, 99 av J-B Clément, 93430 Villetaneuse, France. halpern@math.univ-paris13.fr
[3] Laboratoire de mathématiques Bât 405, Université Paris 11, 91405 Orsay, France. Stephane.Labbe@math.u-psud.fr

**Summary.** We present an optimized Schwarz waveform relaxation algorithm for the parallel solution in space-time of the equations of ferro-magnetics in the micro-magnetic model. We use Robin transmission conditions, and observe fast convergence of the discretized algorithm. We show numerically the existence of an optimal parameter in the Robin condition, and study its dependence on the various physical and numerical parameters.

## 1 Introduction

Over the last decades, ferro-magnetics has been the subject of renewed interest due to its omnipresence in industrial applications, and the need for correctly predicting the behavior of ferro-magnets, which is best achieved by numerical simulations, see the historical introduction in [11] and [1]. Since micro-magnetic simulations are very costly, we present in this paper an optimized Schwarz waveform relaxation algorithm for the micro-magnetic equation. These algorithms have the advantage of independent adaptive discretizations per subdomain both in space and time, and they are naturally parallel, see [6, 7, 4, 5]. We present a numerical analysis of the algorithm with Robin transmission conditions applied to the equation of ferro-magnetics for a two subdomain decomposition, and study the dependence of the optimal parameter on the various physical and numerical parameters.

## 2 The Micro-Magnetic Model

Let $\Omega$ be a bounded open set in $\mathbb{R}^3$ filled with a ferromagnetic material. The magnetic state of the material is given by its magnetization vector $\boldsymbol{m} \in \mathbb{R}^3$,

vanishing outside $\Omega$, with the non-convexity constraint

$$|\boldsymbol{m}| = 1 \text{ a.e. in } \Omega. \tag{1}$$

The behavior of $\boldsymbol{m}$ is modeled by the Landau-Lifschitz equation,

$$\frac{\partial \boldsymbol{m}}{\partial t} = \mathcal{L}(\boldsymbol{m}) := -\boldsymbol{m} \times \boldsymbol{h}(\boldsymbol{m}) - \alpha \boldsymbol{m} \times (\boldsymbol{m} \times \boldsymbol{h}(\boldsymbol{m})), \tag{2}$$

where $\alpha > 0$ is the dissipation parameter. As a first step toward real computations, we include only the exchange interaction, which is local, and produces a magnetic excitation $\boldsymbol{h}(\boldsymbol{m}) = A \triangle \boldsymbol{m}$, where $A > 0$ is the exchange constant. The equation in $\Omega \times (0, T)$ is subject to homogeneous Neumann boundary conditions on the boundary of $\Omega$, i.e. $\frac{\partial \boldsymbol{m}}{\partial \nu} = \boldsymbol{0}$, where $\boldsymbol{\nu}$ is the unit outward normal on the boundary. Equation (2) is often used to compute the steady states of the magnetization field; for more information, see [8].

## 3 Optimized Schwarz Waveform Relaxation Algorithm

We decompose the domain $\Omega$ into $p$ non-overlapping subdomains $(\widetilde{\Omega}_i)_{i=1\ldots p}$, $\bigcup_{i=1}^{p} \overline{\widetilde{\Omega}_i} = \overline{\Omega}$. We then derive from this non-overlapping decomposition an overlapping one by choosing $(\Omega_i)_{i=1\ldots p}$ such that $\widetilde{\Omega}_i \subset \Omega_i$ and $\bigcup_{i=1}^{p} \Omega_i = \Omega$.

We define the interfaces and exterior boundary by

$$\Gamma_{ij} = \partial\Omega_i \cap \overline{\widetilde{\Omega}_j}, \qquad \Gamma_i^e = \partial\Omega_i \cap \partial\Omega.$$

An optimized Schwarz waveform relaxation algorithm computes for $n = 1, 2, \ldots$ the iterates $(\boldsymbol{m}_i^n)_{1 \le i \le p}$ defined by

$$\begin{aligned}
\frac{\partial \boldsymbol{m}_i^n}{\partial t} &= \mathcal{L}(\boldsymbol{m}_1^n) && \text{in } \Omega_i \times (0, T), \\
\boldsymbol{m}_i^n(\cdot, 0) &= \boldsymbol{m}_0 && \text{on } \Omega_i, \\
\mathcal{B}_{ij} \boldsymbol{m}_i^n &= \mathcal{B}_{ij} \boldsymbol{m}_j^{n-1} && \text{on } \Gamma_{ij} \times (0, T), \\
\frac{\partial \boldsymbol{m}_i^n}{\partial \boldsymbol{\nu}} &= \boldsymbol{0} && \text{on } \Gamma_i^e \times (0, T),
\end{aligned} \tag{3}$$

where the $\mathcal{B}_{ij}$ are linear operators.

In [2, 5], several strategies for choosing these boundary operators are proposed both in the case with and without overlap, and a complete convergence analysis is provided for a linear advection-diffusion equation. Here, because of the non-linearity, such an analysis is not yet available, and we use for our numerical study for the non-overlapping case Robin transmission conditions, which are robust and easy to implement, *i.e.* $\mathcal{B}_{ij} = \frac{\partial}{\partial \boldsymbol{\nu}} + \beta_{ij}\mathrm{I}$, where $\beta_{ij}$ is a positive real number to be chosen optimally for best convergence.

## 4 Discretization

We use in space a finite difference discretization on a regular rectangular grid, where the Laplace operator can be approximated by the standard five point finite difference stencil. Since we use cell-centered nodes, the boundaries and the interfaces are halfway in between two nodes, and hence values there can be approximated using the mean of the two adjacent nodes, denoted by $A$ and $B$ in Figure 1, whereas the normal derivative can be approximated by a finite difference between the same nodes $A$ and $B$.

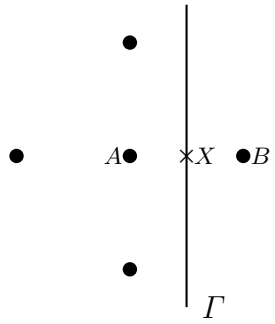


**Fig. 1.** Position of the interface in our cell-centered finite difference discretization.

The Robin condition $\partial_{\boldsymbol{\nu}}\boldsymbol{m} + \beta\boldsymbol{m} = g$ at point $X$ in Figure 1 is thus discretized by $\frac{\boldsymbol{m}_B - \boldsymbol{m}_A}{\Delta x} + \beta\frac{\boldsymbol{m}_A + \boldsymbol{m}_B}{2} = g$, where $\Delta x$ is the space step-size. This yields $\boldsymbol{m}_B = (2\Delta x g + (2 - \beta\Delta x)\boldsymbol{m}_A)/(2 + \beta\Delta x)$, which is then used to complete the missing value at the node $B$ in the five-point finite difference stencil centered at $A$ in Figure 1.

For the time discretization, we use the explicit second order scheme from [9, 10],

$$\boldsymbol{m}_{i+1} = \boldsymbol{m}_i + \Delta t\boldsymbol{F}(\boldsymbol{m}_i) + \frac{\Delta t^2}{2}\mathrm{D}\boldsymbol{F}(\boldsymbol{m}_i)\cdot\boldsymbol{F}(\boldsymbol{m}_i), \tag{4}$$

where D is the differentiation operator and

$$\boldsymbol{F}(\boldsymbol{m}_i) = -\boldsymbol{m}_i \times \boldsymbol{h}(\boldsymbol{m}_i) - \alpha\boldsymbol{m}_i \times (\boldsymbol{m}_i \times \boldsymbol{h}(\boldsymbol{m}_i)).$$

To satisfy the non-convexity constraint (1), we renormalize the magnetization after each time step. Our implementation can use an optimized time step per subdomain in order to maximize energy dissipation and speed up convergence to the steady state, and thus the algorithm is truly non-conforming in time. To study however the convergence to the discrete solution on the entire domain $\Omega$ numerically, we use in the sequel fixed time steps in the subdomains.

## 5 Numerical Study of the Algorithm

We consider a squared ferromagnetic thin plate of dimension $3.68e{-}6 \times 3.68e{-}6 \times \Delta x$, with the parameter $A = 4.06e{-}18$. We also fix the parameter $\alpha$ to be $\frac{1}{2}$.

We divide the domain into two subdomains, as shown in Figure 2. In this non-overlapping case, $\Gamma_{12} = \Gamma_{21} = \Gamma$, and we consider the case $\beta_{12} = \beta_{21} = \beta$ only. We discretize the problem as shown in Section 4, and we first compute

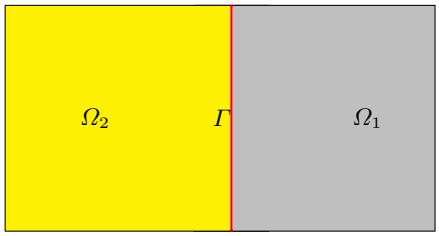


**Fig. 2.** The two subdomain decomposition used for our numerical experiments.

the discrete solution on the entire domain. We then measure the relative error between the mono-domain solution and each iteration of the optimized Schwarz waveform relaxation algorithm in the $l_h^2$ norm,

$$\|\boldsymbol{u}\|_{l_h^2}^2 = \sum_{i=1}^{N} |\omega_i| |\boldsymbol{u}_i|^2.$$

Since $(\omega_i)$ is a rectangular mesh, $|\omega_i| = |\Delta x|^3$.

We mesh the ferromagnetic domain with a space step of $\Delta x = 1.84e{-}7$, which yields a $20 \times 20 \times 1$ mesh. A numerical experiment over long time shows that for the physical parameters chosen above, the equilibrium state has not yet been reached at $T = 30000$.

We first study the convergence behavior of the optimized Schwarz waveform relaxation algorithm. The simulations presented here are done without overlap. We choose a final time of $T = 500$, and perform a series of computations for fixed $\Delta t$, for various values of the parameter $\beta$. In Figure 3, we show for the time discretization steps $\Delta t = 0.125$ and $\Delta t = 5$ the relative error curves for a sequence of iterates as a function of the parameter $\beta$ in the Robin transmission condition. The algorithm is convergent, and there is a numerically optimal choice $\beta_{opt}$ for $\beta$: in both cases, $\beta_{opt} \approx 1.05e{+}7$, which indicates that $\beta_{opt}$ does not depend on the time step.

We now study the dependence of $\beta_{opt}$ on the space discretization step $\Delta x$. As the step size increases, $\beta_{opt}$ in the Robin transmission conditions decreases. The least squared best fit shown in Figure 4 gives $\ln \beta_{opt} \approx 1.03 - 0.97 \ln(\Delta x)$, which indicates that

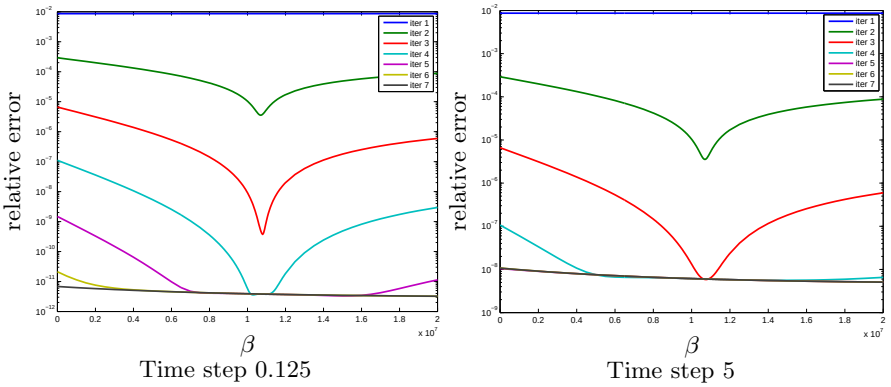


**Fig. 3.** Convergence curves as function of the optimization parameter $\beta$ for two different time steps.

$$\beta_{opt} \approx \frac{2.8}{\Delta x}. \tag{5}$$

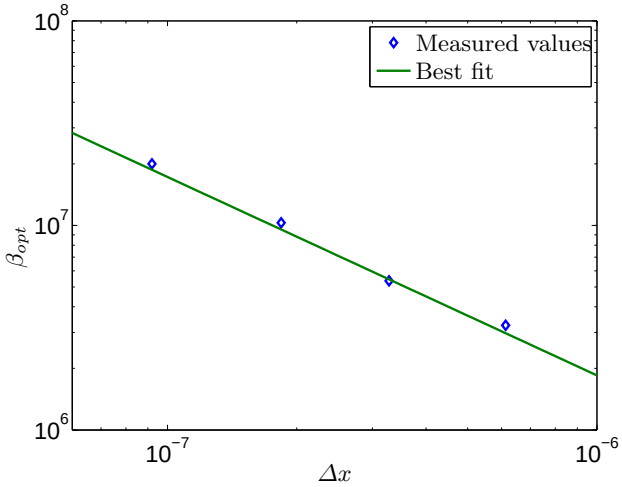


**Fig. 4.** $\beta_{opt}$ as a function of the space discretization step

In the next sequence of numerical experiments, we study the dependence of $\beta_{opt}$ on the physical parameters of the problem. In Figure 5, we show for the final times $T = 100$ and $T = 4000$ the relative error curves for a sequence of iterations as a function of the parameter $\beta$ in the Robin transmission condition. These results, and a large sample of final times between 1 and 4000 indicate that $\beta_{opt}$ does not seem to depend on the final time. This is somewhat

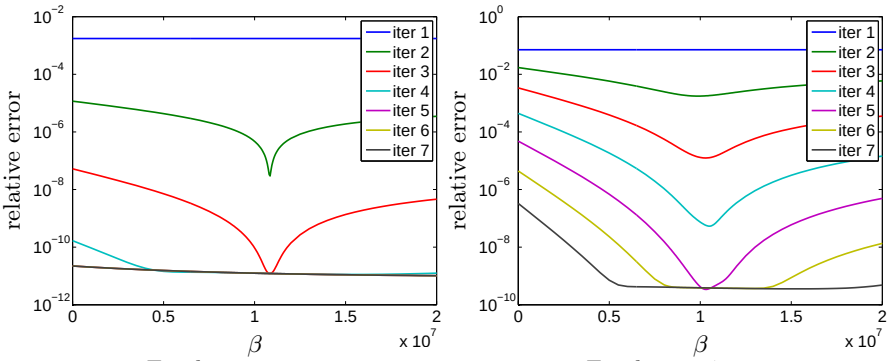


**Fig. 5.** Convergence curves as function of the optimization parameter for two final times.

unexpected, since for the linear heat equation, $\beta_{opt}$ depends on the final time, see [3].

The fact that $\beta_{opt}$ does not depend on the final time of the simulation implies that $\beta_{opt}$ does not depend on the physical parameter $A$ in our case, since dividing the entire equation by $A$ shows that $A$ can be interpreted as a scaling factor for the final time. If however other exchange interactions were present, such as the demagnetization field, this scaling argument would not hold any more.

It remains to study the behavior of $\beta_{opt}$ when $\alpha$ varies. To this end, we compute the convergence curves with parameters $T = 200$ and $\Delta x = 1.84e{-}7$ for $\alpha$ ranging from 0.1 to 100. We present some of these results in Figure 6. For small $\alpha$, the algorithm converges very well and the $\beta_{opt}$ has an approximate value of $1.05e{+}7$. However as $\alpha$ increases, the value of $\beta_{opt}$ varies as shown in Figure 7 and the optimal error increases, see Figure 7.

## 6 Conclusion

We presented an optimized Schwarz waveform relaxation algorithm for the equations of ferro-magnetics in the micro-magnetic model. We studied numerically the convergence behavior of the algorithm with Robin transmission conditions. This study revealed that the algorithm converges very fast: after only few iterations, an error reduction by a factor of $10^{-9}$ is achieved. Using extensive numerical results, we determined a heuristic formula for the value of $\beta_{opt}$, in the non-overlapping case,

$$\beta_{opt} \approx \frac{g(\alpha)}{\Delta x},$$

where $g(\alpha)$ is represented in Figure 7 on the left.

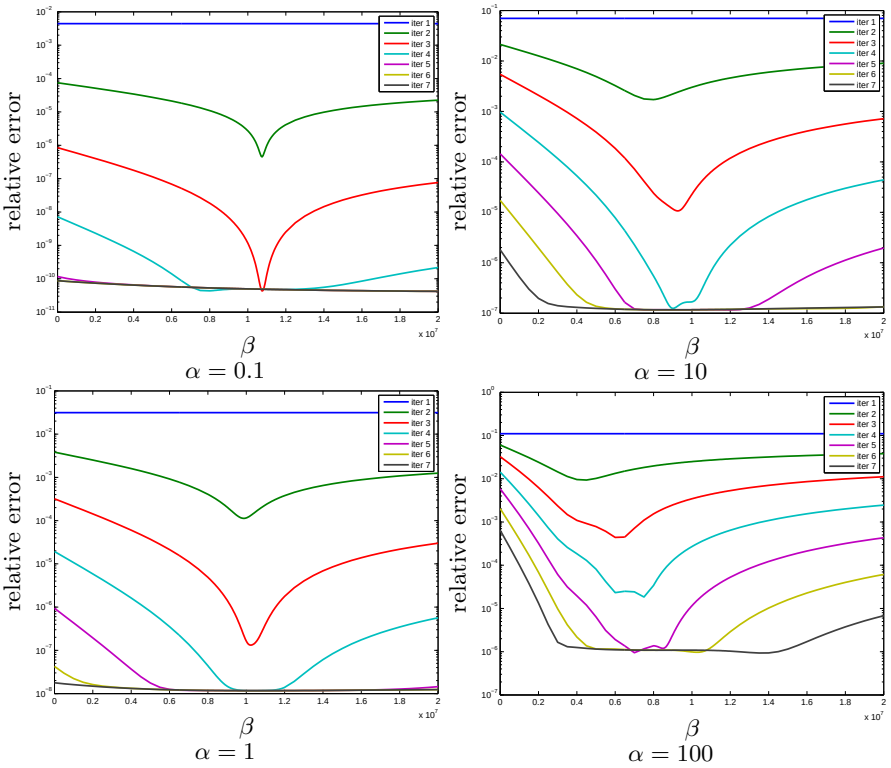


**Fig. 6.** Convergence curves for various choice of $\alpha$

.

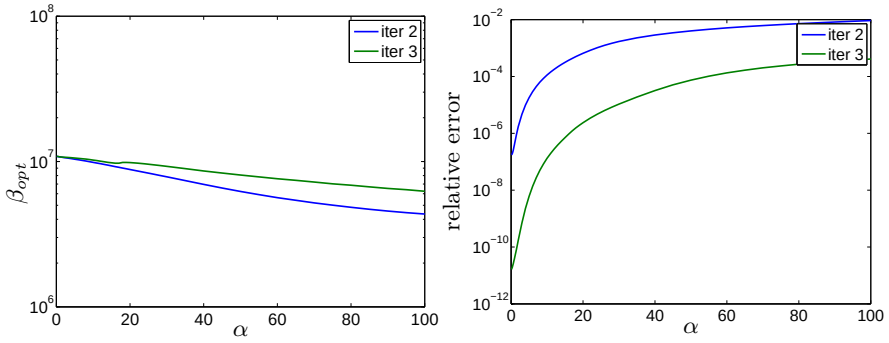


**Fig. 7.** $\beta_{opt}$ and optimal error as functions of $\alpha$

We are currently working on a convergence analysis of the algorithm, and the extension to other interaction terms; in particular adding the demagnetization field interaction is challenging, since it represents a global operator.

## References

[1] A. Aharoni. *Introduction to the Theory of Ferromagnetism*. Oxford Science Publication, 1996.

[2] D. Bennequin, M.J. Gander, and L. Halpern. Optimized Schwarz waveform relaxation methods for convection reaction diffusion problems. Technical Report 24, Institut Galilée, Paris XIII, 2004.

[3] M.J. Gander and L. Halpern. Méthodes de relaxation d'ondes (SWR) pour l'équation de la chaleur en dimension 1. *C. R. Math. Acad. Sci. Paris*, 336(6):519–524, 2003.

[4] M.J. Gander and L. Halpern. Absorbing boundary conditions for the wave equation and parallel computing. *Math. Comp.*, 74(249):153–176, 2004.

[5] M.J. Gander and L. Halpern. Optimized Schwarz waveform relaxation methods for advection reaction diffusion problems. *SIAM J. Numer. Anal.*, 45(2):666–697, 2007.

[6] M.J. Gander, L. Halpern, and F. Nataf. Optimal convergence for overlapping and non-overlapping Schwarz waveform relaxation. In C-H. Lai, P. Bjørstad, M. Cross, and O. Widlund, editors, *Eleventh International Conference of Domain Decomposition Methods*, pages 27–36. ddm.org, 1999.

[7] M.J. Gander, L. Halpern, and F. Nataf. Optimal Schwarz waveform relaxation for the one dimensional wave equation. *SIAM J. Numer. Anal.*, 41(5):1643–1681, 2003.

[8] L. Halpern and S. Labbé. La théorie du micromagnétisme. Modélisation et simulation du comportement des matériaux magnétiques. *Matapli*, 66:77–92, September 2001.

[9] S. Labbé. *Simulation Numérique du Comportement Hyperfréquence des Matériaux Ferromagnétiques*. PhD thesis, Université Paris 13, Décembre 1998.

[10] S. Labbé and P.-Y. Bertin. Microwave polarizability of ferrite particles. *J. Magnetism and Magnetic Materials*, 206:93–105, 1999.

[11] É. Trémolet de Lacheisserie, editor. *Magnétisme: Fondements*, volume I of *Collection Grenoble Sciences*. EDP Sciences, 2000.